Thermoelastic equation of state of molybdenum

Yusheng Zhao,[1] Andrew C. Lawson,[1] Jiangzhong Zhang,[2] Bard I. Bennett,[1] and Robert B. Von Dreele[1]
[1]*LANSCE, Los Alamos National Laboratory, Los Alamos, New Mexico 87545*
[2]*CHiPR, State University of New York, Stony Brook, New York 11794*
(Received 3 August 1999; revised manuscript received 27 April 2000)

We report some high *P-T* diffraction experimental results on molybdenum using synchrotron x-ray and time-of-flight neutron-diffraction techniques. Unit-cell dimensions, measured up to $P=10$ GPa and $T=1475$ K, were derived from the refinement results and fitted to a high-temperature third-order Birch-Murnaghan equation of state. The derived thermoelastic parameters for molybdenum are: isothermal bulk modulus $K_{T0}=266(9)$ GPa with a pressure derivative of bulk modulus $\partial K/\partial P=4.1(9)$, temperature derivative of bulk modulus $\partial K/\partial T=-3.4(9)\times10^{-2}$ GPa/K, volumetric thermal expansivity $\alpha=a+bT$ having $a=1.32(14)\times10^{-5}$ K^{-1} and $b=1.26(15)\times10^{-8}$ K^{-2}. Further, all of the previous experimental data involving shock wave, ultrasonic, thermal-expansion measurements were also analyzed and fitted to a high-temperature Birch/Vinet equation of state (EOS) and the thermal pressure approach of Mie-Grüneisen EOS, respectively. With the greatly extended *P-V-T* data coverage, we refined the thermoelastic parameter set for molybdenum as isothermal bulk modulus $K_{T0}=268(1)$ GPa with pressure derivatives of bulk modulus $\partial K/\partial P=3.81(6)$, $\partial K^2/\partial P^2=-1.41(13)\times10^{-2}$, temperature derivative of bulk modulus $\partial K/\partial T=-2.13(31)\times10^{-2}$ GPa/K, volumetric thermal expansivity $\alpha=a+bT$ having $a=1.31(10)\times10^{-5}$ K^{-1} and $b=1.12(11)\times10^{-8}$ K^{-2}, and an invariant of $\alpha K_T=5.43(5)\times10^{-3}$ GPa/K over a wide *P-T* range. We have conducted a neutron-diffraction study at simultaneous high pressures and high temperatures. Thermal vibrations of atoms (Debye-Waller factors) of molybdenum were derived as a function of pressure and temperature. The experimental results of thermoelastic equation of state parameters are compared with previous experimental data derived from shock wave and ultrasonic elasticity measurements.

INTRODUCTION

Molybdenum is a high technology metal with wide engineering applications for its thermal and mechanical strength, and also chemical resistances. The extreme stability and refractory properties of molybdenum are considered to be associated with its body-centered-cubic (*bcc*) structure (O_h^9-$Im3m$), the result of a high percentage of ''*d* character'' in bonding hybrid orbits. It has been used as corrosion-resistant lining in chemical reactors and as an excellent high strength material applicable at extreme conditions. Molybdenum has a very high melting temperature, $T_m=2893$ K, and the T_m increases with applied pressure.[1] It is observed in acoustic velocity measurements that there is a phase transition of *bcc-hcp* at high shock pressure of 210 GPa and high temperature of 4100 K.[2] However, further investigation by static compression in a diamond-anvil cell up to 420 GPa (Ref. 3) could not confirm this phase transition and much higher transition pressure has been suggested by computational modeling.[4] Molybdenum has been used as flyer and/or back reflector for shock wave experiments to provide certain equation of state references.[5,6] Accurate and precise measurements of its thermoelastic equation of state are critical for theoretical/practical implications.

The thermoelastic equation of state (EOS) is a measure of relationship between pressure, volume, and temperature (*P-V-T*). The inclusion of temperature makes it distinct from the *P-V* equation of state. The term ''thermoelastic'' emphasizes that the final outcomes of the EOS determination are the thermoelastic properties of the matter, such as temperature derivative of bulk modulus and Grüneisen parameters. The thermoelasticity is fundamental behavior of condensed matter and has been applied in the modeling of high-*P-T* phenomena under dynamic shocks[7] and inside the planetary interiors.[8] However, to date, the thermoelastic equations of state, specifically the pressure and temperature derivatives of bulk modulus and thermal expansion, of most metals and ceramics have not been studied in a completed form. Recently, high *P-T* x-ray/neutron-diffraction experiment has been the most important way to derive the thermoelastic EOS. Large-volume high-pressure device running at high temperature plus high intensity synchrotron x-ray and/or time-of-flight neutron-diffraction techniques provide the means to derive thermoelastic EOS, crystal structure, and Debye-Waller factors of the sample materials.

HIGH *P-T* X-RAY AND NEUTRON DIFFRACTION

High-pressure/temperature *in situ* x-ray diffraction of the present study was achieved by integrating a DIA-type cubic-anvil press, the SAM-85 at SUNY Stony Brook, with a synchrotron white radiation source from the superconducting wiggler port X-17B, NSLS, Brookhaven.[9] The energy dispersive spectra of the powder sample were collected with a Ge solid-state detector at a fixed Bragg angle and displayed in real time on a multichannel analyzer. The relationship between diffraction energy, which gives the *d* spacing, and recording channels was calibrated using the γ-radiation standards of Fe^{55}, Co^{57}, Cd^{109}, and I^{129}. The spectra of a mixture of diffraction standards Si, Al_2O_3, and MgO were taken right

before and just after each experimental run to calibrate 2θ and energy. The incident x-ray beam was collimated to a beam dimension of $200\times100\,\mu$m (horizontal by vertical), and the detector optics limited 2θ acceptance angle to 0.006°, which ensures high resolution of the observed diffraction spectra.

Molybdenum powder (Alfa, 99.99% purity) was packed together with NaCl powder mixture in a cylindrical hexagonal boron nitride *h*BN sample chamber of 1 mm in diameter and 2 mm in length. NaCl serves as the pressure standard[10] as well as the pressure medium. We purposely introduce a big volumetric ratio (~70%) of NaCl in the sample mixture so as to reduce the x-ray opaqueness of the heavy metal Mo. The cylindrical *h*BN sample chamber was placed in an amorphous carbon heater and embedded in a boron-epoxy cube to form the high-*P*-*T* cell assembly. With our miniature diffraction optics and relatively high 2θ angle ($2\theta=8.510°$) only sample diffraction at high-*P*-*T* conditions was observed and total elimination of diffraction from the *h*BN sample chamber was achieved. The sample temperature of the high-pressure/temperature cell assembly was monitored using a W/5%Re-W/26%Rh thermocouple (C-type, Omega Engineering, Inc.) and was controlled by a dc power supply. For the high-*P*-*T* experiments the temperature was stable to within 2 °C over the time period of several hours and was constant to within 5 °C in the sample volume.[9] Pressures for the sample were all calculated from the lattice constants of the NaCl pressure calibrant and were estimated to be accurate within $\Delta P=\pm0.1$ GPa.

Significant deviatoric stress is applied to the sample during the initial ''cold'' compression stage, which is indicated by the remarkable broadening of the diffraction peaks.[9,11] Upon heating, deviatoric stress in the sample decreases as the temperature rises. The quasihydrostatic condition can be attained when yield strength of the material drops drastically at high temperatures and plastic flow occurs in the sample and surrounding cell. The yield strength of the refractory metal is quite high and quasihydrostatic condition can only be achieved by softening of NaCl and *h*BN sample chamber. The total yield of NaCl at high temperatures was verified by comparing the peak width [full width at half maximum (FWHM)] of the diffraction spectra. We used a *P*-*T* path (Fig. 1) that the initial compression slightly exceeded the highest desired pressure, and then the whole cell assembly was heated to the highest desired temperature. Those data points collected during the cold compression stage involved severe deviatoric stress and were not included in the lattice refinement. Quasihydrostatic conditions during the experiment were achieved because of (i) large volume proportion of the NaCl (~70%) in the sample mixture, (ii) high-temperature creeping of NaCl pressure medium and *h*BN cell assembly, (iii) refinements of diffraction data only for those of decompression and cooling. The peak width for molybdenum and NaCl observed at high-*P*-*T* conditions were about same as those observed at ambient conditions, a good indication of quasihydrostatic condition.[3] The deviatoric stress on sample is estimated to be σ_1-$\sigma_3\leqslant0.3$ GPa at high pressure and room temperature and it decreases to a level of less than 0.02 GPa at high temperatures of $T\geqslant800$ K.[9]

A diffraction spectrum of molybdenum at elevated pressures and temperatures is compared with the diffraction collected at ambient conditions in Fig. 2 to show the quality of diffraction data. Only those *P*-*V*-*T* data collected at quasihydrostatic compression conditions, as listed in Table I and plotted in Fig. 3, were used to derive the thermoelastic parameters. We ran a le Bail profile refinement[12] for synchrotron x-ray-diffraction data using general structure analysis system (GSAS).[13] Structure and thermal factors are extracted

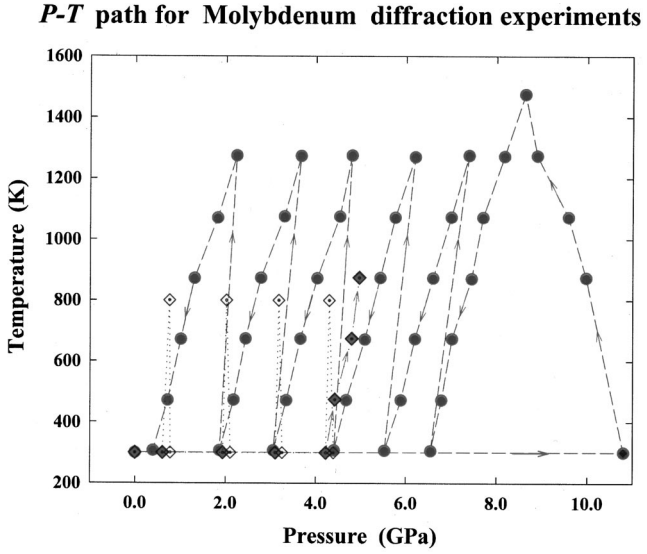

FIG. 1. The *P*-*T* path for diffraction study of molybdenum. The quasihydrostatic compression conditions are achieved at the high temperature and remain so for the decompression and cooling steps. The circular symbols are for synchrotron x-ray data and diamond symbols are for time-of-flight neutron data. The empty diamond symbols are to indicate preheating processes before the neutron data collection. Only those *P*-*V*-*T* data collected at quasihydrostatic compression conditions are used to derive the thermoelastic parameters.

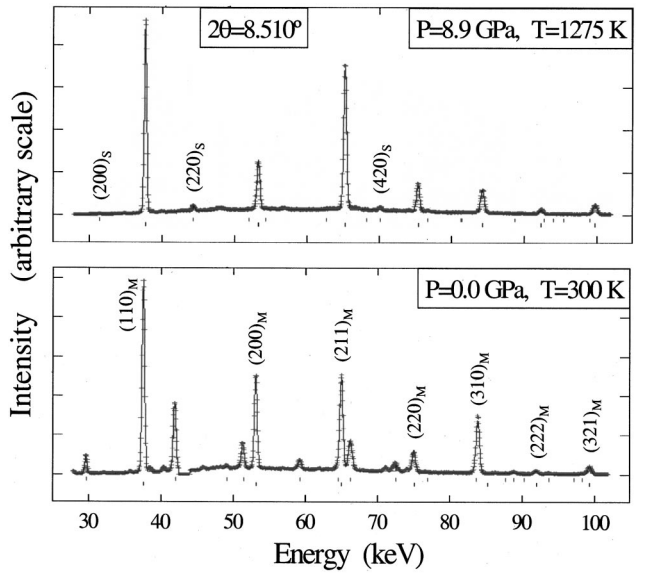

FIG. 2. High-*P*-*T* synchrotron x-ray diffraction of molybdenum (marked with subscript *M*) and NaCl (marked with subscript *S* for salt). The similar peak width (FWHM) for data collected at ambient conditions and at high-*P*-*T* conditions is a good indication of quasihydrostatic condition for sample.

TABLE I. Cell volumes of molybdenum at high P-T.

P (GPa)	T (K)	V (Å^3)	P (GPa)	T (K)	V (Å^3)
0.00	301	31.150(3)		Neutron diffraction	
10.80	301	29.998(3)		at high-P-T conditions	
9.97	874	30.379(1)			
9.58	1073	30.578(2)	0.00	300	31.181(3)
8.89	1274	30.787(2)	0.61	300	31.105(5)
8.63	1475	30.947(2)	1.94	300	30.946(4)
8.17	1272	30.849(1)	3.11	300	30.834(5)
7.70	1072	30.730(1)	4.23	300	30.687(2)
7.45	871	30.651(2)	4.43	475	30.765(2)
7.02	674	30.588(1)	4.70	675	30.842(5)
6.79	473	30.532(1)	4.97	875	30.939(2)
6.55	306	30.481(1)			
7.39	1275	30.981(3)			
7.00	1073	30.833(2)			
6.60	873	30.734(2)			
6.20	674	30.671(2)			
5.89	473	30.621(3)			
5.53	307	30.567(3)			
6.20	1270	31.066(2)			
5.76	1072	30.958(2)			
5.43	874	30.874(2)			
5.09	672	30.795(2)			
4.68	473	30.729(2)			
4.41	308	30.671(2)			
4.80	1275	31.253(3)			
4.53	1075	31.153(3)			
4.03	872	31.015(4)			
3.66	674	30.950(3)			
3.35	472	30.873(2)			
3.06	307	30.829(3)			
3.67	1273	31.425(3)			
3.30	1075	31.267(3)			
2.78	873	31.170(3)			
2.44	674	31.083(3)			
2.18	473	31.024(3)			
1.87	307	30.955(2)			
2.24	1274	31.542(3)			
1.82	1070	31.494(3)			
1.31	872	31.424(3)			
1.01	672	31.279(4)			
0.72	472	31.209(2)			
0.40	307	31.105(4)			

from the refinement of energy dispersive spectra using le Bail's technique. Peak positions and lattice parameters of the diffraction spectra are refined simultaneously for multiple phases. The fitting of the diffraction profile is achieved by least-squares minimization of the differences between the observed pattern and a synthetic pattern. The relative errors of the lattice parameters are determined to be less than 0.02% in all refinement results. Accordingly, the absolute error in the pressure determination is about $\pm 0.04 \sim \pm 0.06$ GPa for the high-pressure/temperature cell assembly.

The high-P-T neutron-diffraction data were collected on the High Intensity Powder Diffractormeter (HIPL) at the Los Alamos Neutron Science Center (LANSCE). The time-of-flight neutron-diffraction spectra of the powder sample were collected by the detector banks at a fixed Bragg angle of $2\theta = \pm 90°$ for the high-P-T experiments. The powder sample of molybdenum and NaCl mixture was loaded into a specially designed high-P-T ceramic cell assembly[14] for toroidal anvil press and compressed by a Paris-Edinburgh cell.[15] To avoid deviatoric stress on the polycrystalline sample, in our high-P-T neutron-diffraction experiments, we always preheat the powder sample to 800 K at each increment in pressure for about 3–5 min, empty diamond symbols

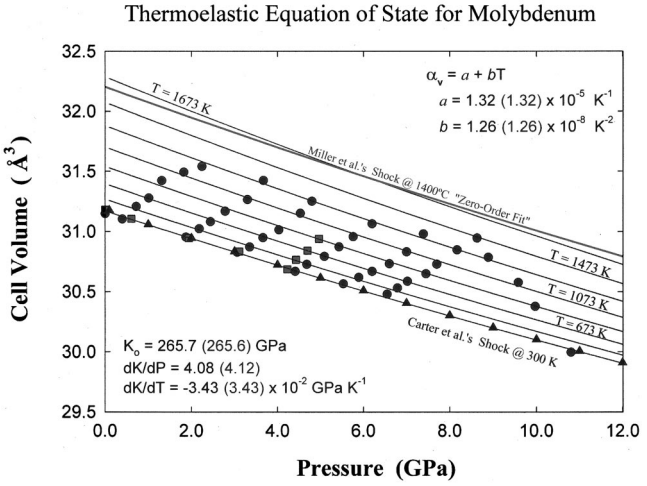

FIG. 3. Cell volumes of molybdenum observed at high-P-T conditions are plotted as a function of pressure. Fitted isothermal compressions are in $\Delta T = 200$ K steps from $T = 473$ K up to $T = 1673$ K. The circular symbols are for syncrotron x-ray-diffraction data and square symbols are for neutron-diffraction data. The triangle symbol is shock experiment data at room temperature (Carter *et al.*, 1971) which falls nicely on the $T = 300$ K isotherm of the present study. The shaded line next to the $T = 1673$ K isotherm compression is EOS fit of shock experiments at $T = 1400\,^{\circ}$C (Miller *et al.*, 1988, *zero-order fit*). The thermoelastic parameters listed are for high-T Birch-Murnaghan EOS and those in parentheses are for high-T Vinet ''universal'' EOS. Two high-T EOS fitting curves overlap perfectly.

in Fig. 1. At this temperature, the NaCl (in a multilayer stack mixed with molybdenum) becomes very soft and the stress field applied to the sample reaches a quasihydrostatic pressure condition at high temperature. We took care in the packing of the powder sample and pressure calibrant mixture to avoid further uncertainty in the pressure measurement. It has been demonstrated that a pressure reading from a powder mixture of hard and soft materials can be quite different. The so-called Lamé effect in the powder mixture makes the hard material experience noticeably higher stress than the soft material,[16] even if the total yield occurs in the soft material. We used a multilayer packing scheme to achieve the ''iso-(P,T)'' condition for both sample and pressure calibrant.[14] The layered packing of powder mixture is also essential for metallic samples to prevent electrical shorts between the heating elements, since the protection tube between sample and furnace is sometimes eliminated in order to have more sample volume and less diffraction contamination from the surroundings. A particular routine to correct diffraction optics and to determine P-V-T was taken for the data reduction.[17] Eight data points of unit-cell volumes collected by high-P-T neutron-diffraction technique are listed in Table I and plotted in Fig. 3 as square symbols.

HIGH-TEMPERATURE EQUATION OF STATE

Based on finite-strain theory, Murnaghan[18] and Birch[19] have derived an equation of state that is independent of bonding character and interatomic potentials to describe isothermal compression. The so-called Birch-Murnaghan EOS is now recognized as empirically the best and widely applied in high-pressure geophysics:

$$P = 3K_0 f(1+2f)^{5/2}[1 + Af + Bf^2], \tag{1}$$

where $A = 3/2(K' - 4)$, $B = 9/6[K_0 K'' + K'(K' - 7)] + 143/6$ and $f = 1/2[(V_0/V_P)^{2/3} - 1]$ is the Eulerian strain,

$$K = -V(\partial P/\partial V)_T, \quad K' = \partial K/\partial P, \quad K'' = \partial^2 K/\partial P^2.$$

Later, Vinet *et al.* proposed that the isothermal pressure-volume (P-V) relations for a wide variety of matters can be accurately described by the ''universal equation of state:'' [20,21]

$$P = 3K_0(1+x)x^{-2}\exp\left[\frac{3}{2}(K'-1)(1-x)\right], \tag{2}$$

where $x = (V_P/V_0)^{1/3}$ is simply the linear compression.

This EOS is based on the universal relationship between binding energy and the interatomic separation. Thermal contribution to the pressure arises at high temperatures as the entropy of the system increases. Many approaches have been proposed on equation of state to deal with thermal effects so as to process P-V-T data. We apply two widely employed methods, namely high-T EOS and thermal pressure approach, to derive thermoelastic parameters from P-V-T data of molybdenum.

One practical way is to introduce temperature effects in a modify equation of state to fit the P-V-T data.[22,23] The high-T EOS modeling first heats the ambient volume V_0 to high temperature isobarically along $P = 0$ and then compress the expanded volume $V(0,T)$ along an isotherm to reach the $V(P,T)$. The following two essential modifications are made to Eq. (1) and/or Eq. (2) to obtain high-T EOS so that the temperature effects are accounted for:

(i) To replace V_0/V_P with V_T/V_{PT}, where V_0 is cell volume at ambient conditions, $V_T = V(0,T)$ at high-T, $V_P = V(P,300\,\mathrm{K})$ at high P, and the observed $V_{PT} = V(P,T)$ at simultaneous high P-T conditions. The V_T can be obtained from isobaric thermal expansion at atmospheric pressure: $V_T = V_0 \exp(\alpha dT)$ and $\alpha = \alpha(0,T) = a + bT - c/T^2$.[24] The Eulerian strain in high-T Birch EOS is thus written as $f = \frac{1}{2}[(V_T/V_{PT})^{2/3} - 1]$, and the linear compression in high-T Vinet EOS is written as $x = (V_{PT}/V_T)^{1/3}$.

(ii) To replace K_0 with K_T, where K_0 is bulk modulus at ambient conditions and K_T is isothermal bulk modulus at high temperatures: $K_T = K_{T_0} + \dot{K}(T - 300)$ and $\dot{K} = \partial K/\partial T$ is the temperature derivative of the bulk modulus. The high-T bulk modulus K_T is applied to reduce V_T to V_{PT} in an isothermal compression.

One may further modify EOS with temperature effects on high-order derivatives, such as $\partial^2 K/\partial P\partial T, \partial^2 K/\partial T^2$, etc. However, such further modifications are usually limited by experimental P-T range and become impractical in most cases. With the limited P-T coverage and a quite small volumetric compression ($\Delta V_{\max}/V_0 < 4\%$) of the molybdenum sample in present study, we ignore the c/T^2 term in thermal expansion and high-order derivatives of the bulk modulus K'', $\ddot{K}$, and $\dot{K}'$. It is important to indicate that, when fitting the equation of state parameters, the $V(P,T)$ data should be independent of the P-T path. Therefore we are able to apply

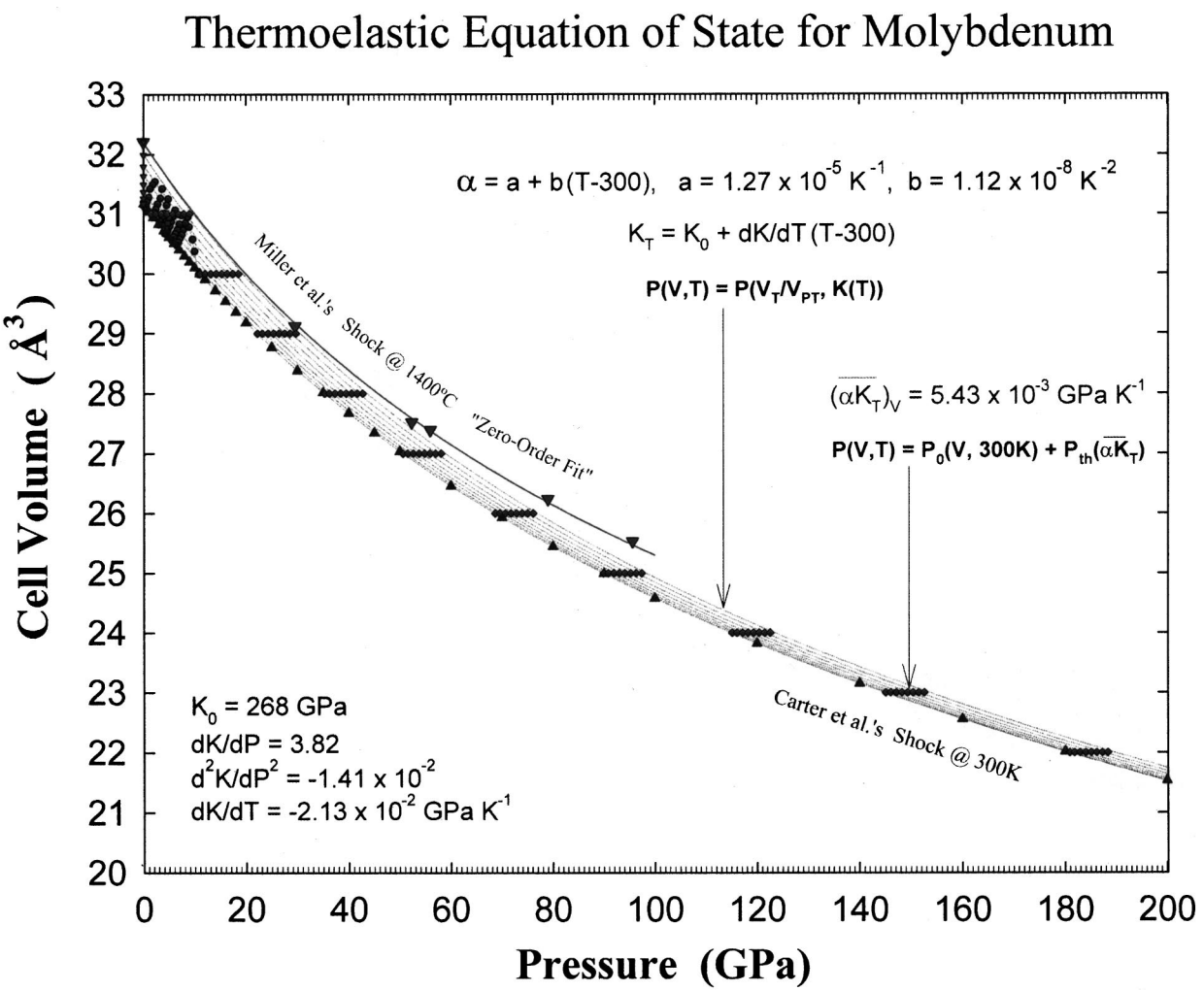

FIG. 4. All experimental data of molybdenum observed at high-P-T conditions are plotted as a function of pressure. The inverted triangles along the y axis of $P=0.0$ GPa represent thermal-expansion data observed at atmospheric pressure. The circular symbols are for synchrotron x-ray-diffraction data and square symbols are for neutron-diffraction data observed at simultaneous high P-T. The triangle symbol is shock experiment data at room temperature (Carter *et al.*, 1971) which falls nicely on the $T=300$ K isotherm of the present study. The inverted triangles are for shock data at $T=1400\,^{\circ}$C and the line is the *zero-order fit* of Miller *et al.* (1988). The thermoelastic parameters listed are for high-T Birch EOS and for thermal pressure approach of Mie-Grüneisen EOS, respectively. The high-T EOS isothermal compression lines are drawn for the experimental pressure range up to $P=200$ GPa, in a temperature step of $\Delta T=200$ K from $T=473$ K to $T=1673$ K. The diamond symbols represent P-V-T data calculated from the isochoric heating on the basis of $T=300$ K isothermal compression. The results from two different approaches, (i) isobaric heating ($P=0.0$ GPa) followed by isothermal compression and (ii) isothermal compression ($T=300$ K) followed by isochoric heating, matches one another within 2% over the whole experimental P-T range.

the ''global fit'' to process all observed P-V-T data simultaneously, even though the experimental data were taken along isotherms.

Thermoelastic parameters for molybdenum are derived by global fitting of the P-V-T data (Table I) to the high-T Birch-Murnaghan EOS [truncated to third order, i.e., $B=0$ in Eq. (1)] and to high-T Vinet EOS, respectively. The derived parameters from these two EOS are essentially identical for the P-V-T data coverage of the present high-P-T diffraction study. The isothermal bulk modulus is $K_{T0}=266(9)$ GPa and pressure derivative of bulk modulus $K'=\partial K/\partial P=4.1(9)$, temperature derivative of bulk modulus $\dot{K}=\partial K/\partial T=-3.4(9)\times10^{-2}$ GPa/K, volumetric thermal expansivity $\alpha=a+bT$ with values of $a=1.32(14)\times10^{-5}\,\mathrm{K}^{-1}$ and $b=1.26(15)\times10^{-8}\,\mathrm{K}^{-2}$. Figure 3 plots the cell volumes as a function of pressure together with the isothermal compression lines calculated from the fitted thermoelastic parameters for high-T Birch-Murnaghan EOS and for high-T Vinet EOS, respectively. The diagram clearly shows that the thermoelastic parameters derived in the present study produce good fits to the P-V-T data of molybdenum and two high-T EOS, high-T form of Eqs. (1) and (2), overlap perfectly.

Numerous experiments have been done on molybdenum including shock wave experiments at room temperature[5] and at high temperature,[28] ultrasonic measurements of elastic constants at high temperatures,[29–31] and thermal-expansion measurements at atmospheric pressure.[32,33] The shock wave experiment at room temperature has reached an ultrahigh pressure of 200 GPa and a significant volumetric compression of $\Delta V/V_0=32\%$, which provides a very good constrain on the bulk modulus and its pressure derivative. The high-temperature shock wave experiment has reached high pres-

TABLE II. Thermoelastic parameters of molybdenum derived from different experimental data. Thermal expansion: $\alpha_0 = a$, $b = \partial\alpha/\partial T$, $\alpha_{T=300\,\mathrm{K}} = a + bT$ at $T = 300$ K. The parentheses (##) are to show the errors for the derived parameters (from last digit). The Ref. Nos. indicate where the data are derived/quoted from. (Fig. 4B) and (Fig. 4V) stand for the high-*T Birch* EOS fit and high-*T Vinet* EOS fit, respectively. Boldfaced data derived from present study is the preferred data set of thermoelastic parameters of Mo.

Bulk modulus	Thermal expansion	Grüneisen parameter
$K_{T0} = 268(1)$ (Fig. 4B) GPa	**$\alpha_0 = 1.31(10)$ (Fig. 4B) $\times 10^{-5}$ K^{-1}**	**$\gamma = 1.75(22)$ (Fig. 4B)**
264(1) (Fig. 4V)	1.28(11) (Fig. 4V)	1.71(24) (Fig. 4V)
266(9) (Fig. 3)	1.32(14) (Fig. 3)	1.83(38) (Fig. 3)
267 (Ref. 5)	1.45 (Ref. 32)	1.52 (Ref. 28)
261 (Ref. 28)	1.44 (Ref. 33)	1.58 (Ref. 35)
268 (Ref. 29)		1.70 (Ref. 2)
262 (Ref. 30)	**$\alpha_{T=300\,\mathrm{K}} = 1.65(21)$ (Fig. 4B) $\times 10^{-5}$ K^{-1}**	
259 (Ref. 31)	1.63(23) (Fig. 4V)	
273 (Ref. 39)	1.70(29) (Fig. 3)	
	1.52 (Ref. 32)	**$\alpha K_T = 5.43(5)$ (Fig. 4) $\times 10^{-3}$ GPa K^{-1}**
	1.53 (Ref. 33)	(derived from thermal pressure approach for large P-T coverage)
$\partial K/\partial P = 3.81(6)$ (Fig. 4B)	**$\partial\alpha/\partial T = 1.12(11)$ (Fig. 4B) $\times 10^{-8}$ K^{-2}**	
4.05(2) (Fig. 4V)	1.18(12) (Fig. 4V)	
4.1(9) (Fig. 3)	1.26(15) (Fig. 3)	**$\Delta\alpha/\Delta P = -2.97(33)$ (Fig. 7) $\times 10^{-5}$ K^{-1} GPa^{-1}**
3.9 (Ref. 5)	0.25 (Ref. 32)	
	0.29 (Ref. 33)	
$\partial K/\partial T = -2.13(31)$ (Fig. 4B) $\times 10^{-2}$ GPa K^{-1}	**$\partial\alpha/\partial P = -2.97(33)$ (Fig. 4B) $\times 10^{-5}$ K^{-1} GPa^{-1}**	Debye temperature
$-1.72(30)$ (Fig. 4V)	$-2.44(32)$ (Fig. 4V)	
$-3.4(9)$ (Fig. 3)	$-4.81(99)$ (Fig. 3)	**$\Theta_{DW} = 455(8)$ (Fig. 10)**
$-2.1(6)$ (Fig. 5)	$-3.02(62)$ (Fig. 5)	$\Theta_D = 445-474$ (Ref. 30)
-1.21 (Fig. 5) (Ref. 28)	-1.77 (Ref. 28)	
-2.07 (Fig. 3) (Ref. 28)	-3.04 (Ref. 28)	
-1.70 (Ref. 29)	-2.36 (Ref. 29)	
-1.73 (Ref. 30)	-2.52 (Ref. 30)	
-1.63 (Ref. 31)	-2.41 (Ref. 31)	
$\partial^2 K/\partial P^2 = 1.41(13)$ (Fig. 4B) $\times 10^{-2}$		
-4.34 (Ref. 5)		

sure of 96 GPa at $T = 1400\,^\circ$C with volumetric compression of $\Delta V/V_0 = 21\%$, which should also provides a good constrain on the pressure and temperature derivative of the bulk modulus. We have plotted both shock wave data sets on Fig. 3 and found out that the shock data at room temperature lines up very nicely with the isotherm $P(V,300\,\mathrm{K})$ derived from Birch EOS [Eq. (1)] and Vinet EOS [Eq. (2)]. While the ''zero-order fit'' of EOS for Miller *et al.*'s (1988) $T = 1400\,^\circ$C shock data has a signifiant mismatch with the $T = 1673$ K isotherm.

The P-V-T data coverage can be greatly extended by including all of the previous experimental data. Thermoelastic parameters for molybdenum are derived again with global fitting of all P-V-T data (Fig. 4) to the high-T Birch EOS (*full expression*) and to high-T Vinet EOS, respectively. The derived isothermal bulk modulus is (Birch EOS−Vinet EOS) $K_{T0} = 268(1) - 264(1)$ GPa; the pressure derivative of bulk modulus $K' = \partial K/\partial P = 3.81(6) - 4.05(2)$, and double pressure derivatives $\partial^2 K/\partial P^2 = -1.41(13) \times 10^{-2}$; temperature derivative of bulk modulus $\dot{K} = \partial K/\partial T = -2.13(31) - 1.72(30) \times 10^{-2}$ GPa/K; volumetric thermal expansivity $\alpha = a + bT$ with values of $a = 1.31(10) - 1.28(11) \times 10^{-5}$ K^{-1} and $b = 1.12(11) - 1.18(12) \times 10^{-8}$ K^{-2}. As shown in the fitting results, Table II, the difference between Birch and Vinet EOS are mostly within three sigma (three times of standard deviation).

THERMAL PRESSURE APPROACH

The thermal pressure approach to process P-V-T data has been widely applied for its thermodynamic significance. In this approach, the sample volume V_0 is first compressed along $T_0 = 300$ K isotherm to V_P and then heated up to high temperature isochorically to $V(P,T) = V(P_0, 300\,\mathrm{K})$. The equations of state (1) and (2) may be followed exactly for the isothermal compression from V_0 to V_P and an additional thermal pressure P_{th} term is introduced to take isochoric heating $(\partial P/\partial T)_V$ into account for constant volume $V_P = V_{PT}$, i.e.,

$$P(V,T) = P(V,300\ \mathrm{K}) + \int_{300}^{T} (\partial P/\partial T)_V dT. \qquad (3)$$

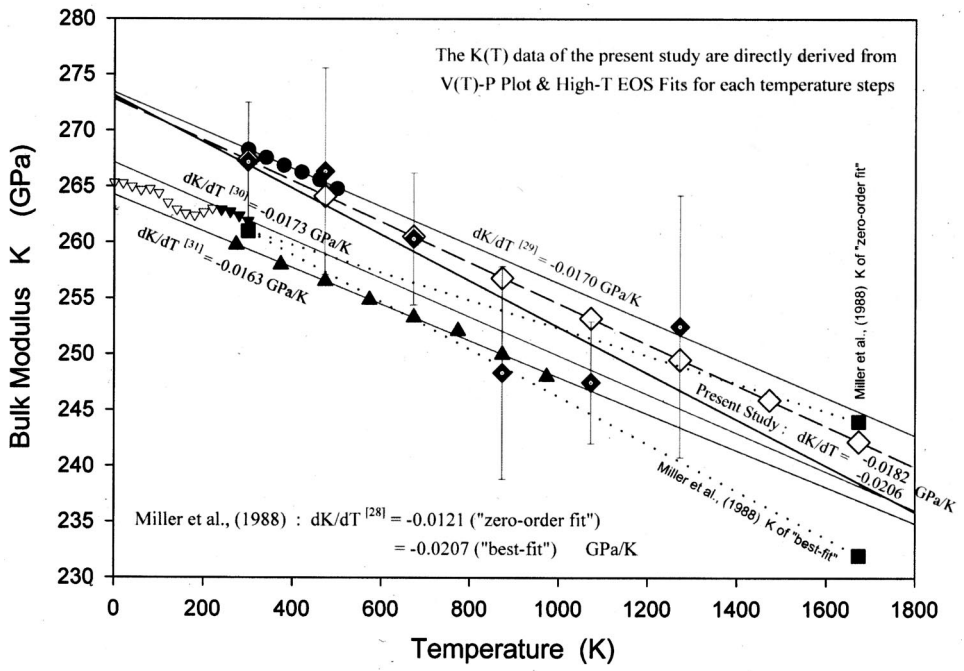

FIG. 5. The bulk modulus of molybdenum plotted against temperature, which shows the ''elastic softening'' effect due to increasing temperature. The filled diamond symbols are bulk modulus derived directly from individual $V(T)$-P plots for each temperature step. The empty diamond symbols are bulk modulus derived from individual high-T EOS fitting curves of each temperature step. The regression result of dK/dT value of the present high-P-T diffraction study is $-0.021(6)$ GPa/K. The dK/dT values derived from different data sets (Ref. No. in bracket) of ultrasonic and shock wave experiments are labeled and placed next to the linear regression lines.

It has been observed experimentally that above Debye temperature Θ_D, thermal pressure $P_{\rm th}$ is a linear function of temperature, i.e., the $(\partial P/\partial T)_V$ in the second term is an invariant in $T>\Theta_D$ high-temperature region.[25,26] Using simple calculus, one may get the invariant of $(\partial P/\partial T)_V = -(\partial V/\partial T)_P/(\partial V/\partial P)_T = \alpha K_T$, and write thermal pressure at constant volume in a rather simple form, $P_{\rm th} = \int_{300}^{T} \alpha K_T dT = \alpha K_r (T-300)$. Thus we get

$$P(V,T) = P(V,300\ \text{K}) + \alpha K_T (T-300). \tag{4}$$

This resembles the Mie-Grüneisen equation of state, with the difference that the first term refers to $T=300$ K isotherm, instead of to $T=0$ K. The thermal pressure approach works over a large P-T range, with substantial compression $\Delta V/V_0$, and for many different materials.[21,26,27] Next, we compare high-T EOS and thermal pressure approaches to see if these two match one another in the P-V-T data analysis. In the mean time, we include all the experimental data performed for molybdenum and greatly expand the P-T coverage of the investigation.

We conducted the global fit using thermal pressure approaches to fit all the data with Eq. (4) to derive isochoric heating effects. The isochoric thermal pressures are plotted in Fig. 4, shown as empty diamond symbols, together with the isothermal compression lines derived from high-T EOS. It is observed that the derived pressures and volumes with these two different approaches match within 2% for the whole P-T range.

We have used the complete formula of the equation of state with higher-order derivatives, to fit the much more enlarged P-V-T data. The present high-P-T synchrotron x-ray and time-of-flight neutron-diffraction experiments occupy only a very small portion in the data space. Nevertheless, they are still greatly valuable in fitting the thermoelastic equation of state. We did not use Miller *et al.*'s (1988) shock wave data at $T=1400\,^\circ$C in the nonlinear regression of the high-T EOS and for the thermal pressure approach, for the reason that it does not have the intrinsic EOS feature presented in the room-temperature shock data. The isotherm of the *zero-order fit* together with five experimental data observed in the $T=1400\,^\circ$C shock wave experiment show a significant concave curvature, which represent a small K, large dK/dP, $|d^2K/dP^2|$, and an unrealistically small dK/dT. It has been considered that the isochoric thermal pressure may not be true invariant over the P-V-T space and additional modification may also be involved. In such case thermal pressure is written as: $P_{\rm th} = \int_{300}^{T} (\partial P/\partial T)_V dT = [\alpha K_T - (\partial K_T/\partial T)_V \ln(V_{PT}/V_0) + \cdots]\cdot(T-300)$. This formula was found to work quite well for many minerals, however, present study indicates that it is not applicable to the metal Mo case.

OTHER THERMOELASTIC PARAMETERS

Furthermore, thermal Grüneisen parameter at ambient conditions, which quantifies the relationship between thermal and elastic properties, can be derived for molybdenum from the refined thermoelastic data with the thermodynamic formula

$$\gamma_{\rm th} = \frac{\alpha_V \cdot K_T}{\rho \cdot C_V}. \tag{5}$$

With $\alpha_{V0} = 1.65(21)\times 10^{-5}\,\text{K}^{-1}$, $K_{T0} = 268(1)$ GPa, and $\rho_0 = 10.23\,\text{g/cm}^3$ plus the isochoric heat capacity $C_V = 24.7$ J/mol/K,[11] the derived thermal Grüneisen parameter of molybdenum is thus: $\gamma_{\rm th} = 1.75(22)$ for ambient conditions. This value is consistent with the derivation of the shock wave experiments: $\gamma = 1.58-1.70$.[2,34,35] We have derived an invariant $\alpha K_T = 5.43(5)\times 10^{-3}$ GPa/K over a wide P-T range using thermal pressure approach. With the high-T EOS parameters derived for molybdenum in present study, one should be able to plot thermal Grüneisen parameter as a function of pressure and temperature if there were such data for specific heat.

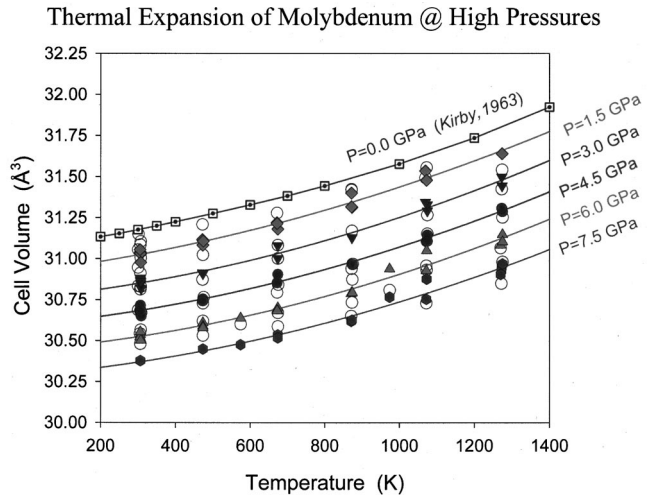

FIG. 6. The cell volumes $V(P,T)$ of molybdenum plotted against temperature. The empty circles represent the raw P-V-T data while filled solid symbols are the corrected cell volumes $V(P_c,T)$ for isobaric $P_c s$ of 1.5, 3.0, 4.5, 6.0, and 7.5 GPa, respectively. Data points in between any two isobaric heating lines are corrected twice to both $P_c s$ (volume up and down corresponds to decompression and compression, respectively). The cell volume data for $P=0.0$ GPa (dotted squares) are derived from Kirby's (1963) thermal expansion data (Ref. 32).

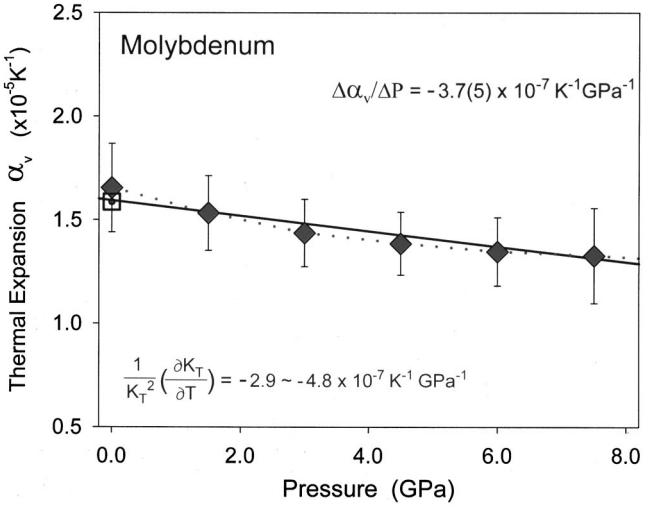

FIG. 7. Thermal expansions of molybdenum plotted as a function of pressure. The diamond symbols represent thermal expansion data derived from Fig. 6 and the dotted square at $P=0.0$ GPa is for Kirby's (1963) thermal expansion data (Ref. 32). The slope of the fitted straight line represents pressure derivative of thermal expansion, $\Delta\alpha/\Delta P$, which is well comparable to the thermodynamic derivation [Eq. (6)].

The change of thermal expansion with pressure is directly related to the change of bulk modulus with temperature. Through the thermodynamic identity,

$$\left(\frac{\partial\alpha}{\partial P}\right)_T=\frac{1}{K_T^2}\left(\frac{\partial K_T}{\partial T}\right)_P. \tag{6}$$

Using the derived thermoelastic parameters, the pressure derivative of thermal expansion for the molybdenum is calculated to be $\partial\alpha/\partial P=-2.97(33)--4.81(99)\times10^{-7}\,\mathrm{K}^{-1}\,\mathrm{GPa}^{-1}$, depending on the choice of P-T range and thermoelastic equation of state. We derive the bulk modulus from individual $V(T)$-P plots and from individual high-T EOS fitting curves for each temperature step, respectively. Plotted in Fig. 5 are bulk moduli as a function of temperature for all experimental data. The regression results of dK/dT of the present high-P-T diffraction study is $-0.021(6)$ GPa/K and the corresponding value of $\partial\alpha/\partial P=-3.02(62)\times10^{-7}\,\mathrm{K}^{-1}\,\mathrm{GPa}^{-1}$. The regression dK/dT values of different data set for ultrasonic[29–31] and shock wave[28] experiments are also derived and shown in Fig. 5.

A different approach can be applied to evaluate this thermodynamic derivation. We plot cell volumes versus temperatures along isobaric heating lines (Fig. 6) in order to derive thermal expansions at different pressures. The raw experimental P-V-T data, as shown by the empty circles, are pretty much lined up in the diagram, although with different pressures. One may correct the raw $V(P,T)$ data to certain constant pressures $P_c s$ to get the isobaric volumes $V(P_c,T)$ using high-T Birch-Murnaghan equation of state. The trick of this correction is to back derive $V(0,T)$ from $V(P,T)$ first and then compress $V(0,T)$ to $V(P_c,T)$. Here, we use the derived thermoelastic parameters: $K_{T0}=266$ GPa; $K'=4.1$; and $\dot{K}=-3.43\times10^{-2}\,\mathrm{GPa\,K}^{-1}$ for the P-T coverage of present study. The solid symbols plotted in Fig. 6 are the corrected $V(P_c,T)$ data for five constant $P_c s$.

The thermal expansions at these five constant pressures can be traced out in the isobaric heating $V(P_c)$-T plot with a second-order linear regressions of $V=b_0+b_1T+b_2T^2$. Thus the thermal expansion $\alpha=a+bT$ has the value $a=(b_1/b_0)$ and $b=(2b_2/b_0)$. We plot the six averaged thermal expansions for temperature range of 300–1300 K against pressure in Fig. 7. It is clearly shown that the volumetric thermal expansion of molybdenum decreases monotonously with increasing pressure. The fitted slope of the straight line is the pressure derivative of volumetric thermal expansion: $\Delta\alpha/\Delta P=-3.7(5)\times10^{-7}\,\mathrm{K}^{-1}\,\mathrm{GPa}^{-1}$. This regression result falls right within the range of thermodynamic derivation

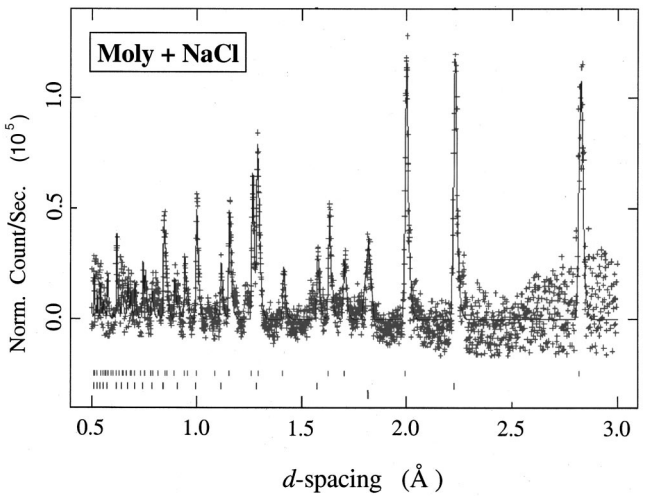

FIG. 8. The time-of-flight neutron-diffraction spectrum of molybdenum and NaCl at simultaneous high-P-T condition. The crosses are the experimental neutron counts and the curve is the Rietveld refinement fit to the experimental data.

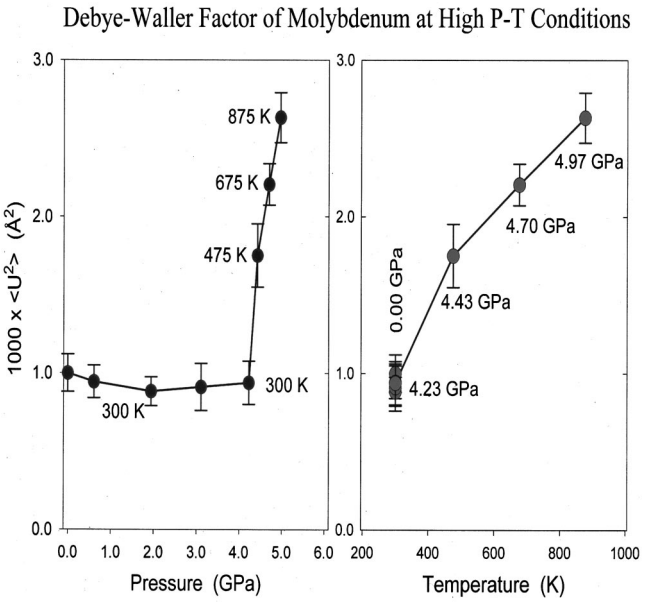

FIG. 9. Normalized (to data collected at ambient conditions) isotropic thermal vibration of molybdenum at high-P-T conditions. The P-T conditions are labeled next to the data points for easy reading of the diagram.

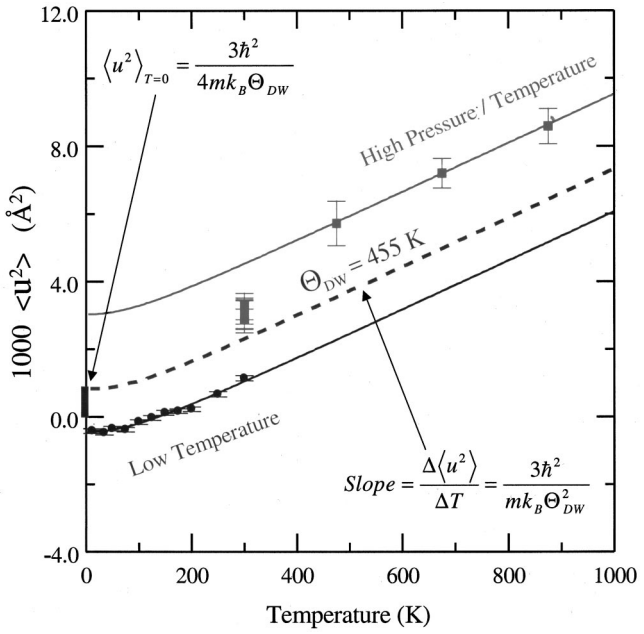

FIG. 10. The isotropic thermal vibration of molybdenum plotted as a function of temperature for two different data sets (present study and Ref. 38). See text for the details of the diagram interpretation.

$\partial\alpha/\partial P = -2.9 \sim -4.8 \times 10^{-7}\,\mathrm{K}^{-1}\,\mathrm{GPa}^{-1}$, two different thermodynamic approaches result in comparable outcomes.

DEBYE-WALLER FACTOR

The Debye-Waller factor is to indicate the thermal vibration of the crystal lattice.[36] The intensity of Bragg diffraction peak decreases as temperature of the crystal increased. The thermal effect is more pronounced at large $Q = |2\pi/d_{hkl}|$ value (higher *hkl*, smaller *d* spacing). The atoms undergo large amplitude random thermal motion with instantaneous nearest-neighbor spacing differing significantly from static positions. For a crystal lattice, the diffraction intensity are weakened by the Debye-Waller factor:

$$DW = e^{-4\pi^2\langle u^2\rangle_{hkl}/d_{hkl}^2}, \tag{7}$$

where $\langle u^2 \rangle$ is the mean-square thermal displacement of an atom from its equilibrium position normal to the plane *hkl* and d_{hkl} is the *d* spacing associated with that plane.

Synchrotron x-ray diffraction in energy dispersive mode does not provide a good intensity calibration at the high P-T conditions. Furthermore, x-ray diffraction, scattering by atomic electrons not nuclei, attenuates significantly at large $Q = |2\pi/d_{hkl}|$ value in a fashion of $|f_e(Q)|^2$ in addition to Debye-Waller factors. Thus it is difficult to apply Rietveld refinement[37] to obtain structural and thermal parameters. The time-of-flight neutron diffraction directly sense the motion of nuclei and the spectra collected (Fig. 8) cover a much large range of scattering vector Q (d spacing down to 0.5 Å!). For only five free parameters involved (lattice and thermal parameters for Mo and NaCl, respectively) plus fitting for background and absorption correction, the neutron-diffraction data are of qualities suitable for Rietveld refinement. The refinement result on isotropic thermal vibration shows significant dependence on temperature, however, not sensitive to pressure. Plotted in Fig. 9 are isotropic thermal parameters as a function of pressure and temperature, respectively. The corresponding pressures and temperatures are labeled next to each data point. As pressure increases up to 4.2 GPa, thermal vibrations of molybdenum atoms were virtually unchanged within the experimental error. The increase of temperature drastically raises up the thermal vibrations of molybdenum atoms. The mean-square thermal displacement $\langle u^2 \rangle$ of the molybdenum atom increases more or less in a linear fashion with temperature as shown in Fig. 9. One may consider the manifest of thermal vibration of atom as an indication of entropy of the system, where temperature dominates the process.

The Debye approximation is applied in discussing the integral vibrational properties of crystals.[36] For a monatomic cubic crystal with Debye frequency distribution, the temperature dependence of mean-square thermal displacement of the atom is written as

$$\langle u^2 \rangle_{\mathrm{ideal}} = \frac{3\hbar^2 T}{mk_B\Theta_{\mathrm{DW}}^2}\left(\frac{1}{4}\frac{\Theta_{\mathrm{DW}}}{T} + \frac{T}{\Theta_{\mathrm{DW}}}\int_0^{\Theta_{\mathrm{DW}}/T}\frac{u\,du}{e^u - 1}\right), \tag{8}$$

where m is the mass of the atom, k_B is Boltzmann's constant, $\hbar$ is Planck's constant and Θ_{DW} is the Debye-Waller temperature, a characteristic temperature of the particular material. Strictly speaking, Θ_{DW} is not identical with the Debye temperature determined from heat-capacity measurement, but their numerical values are generally close.[38] At high temperature, i.e., $T > \Theta_{\mathrm{DW}}$, the $\langle u^2 \rangle$ is proportional to the absolute temperature T. The $\langle u^2 \rangle$ versus temperature curve is thus linear and the slope of the curve is inversely proportional to square of Θ_{DW}. In the low-temperature region, i.e., $T \ll \Theta_{\mathrm{DW}}$, zero-point motion is predominant and independent of temperature. The current thermal vibration data of molyb-

denum observed at high pressures and high temperatures are plotted together with Lawson *et al.*'s low-temperature data in Fig. 10 in order to demonstrate the Debye approximation.

There is an apparent mismatch between two data sets on their absolute values. Also noticed is that both data sets need some corrections to make the measurements meaningful. The low-temperature data have negative values at temperature range $T<100$ K (discussed in Ref. 14 as ''offset'' phenomenon), while high-temperature data have an unusual kink from $T=300$ K to $T>400$ K. The reasons for these effects are not clear to us for now and more experimental studies are needed to exclude the system error. Nevertheless, both data sets can still be fitted with straight lines of similar slopes (Fig. 10). The dashed line drawn in the diagram is the best representative curve of thermal vibration of molybdenum as a function of temperature. The derived Debye-Waller temperature, $\Theta_{\mathrm{DW}}=455(8)$ K, is inversely proportional to the square root of the fitted slope of the curve at high-temperature portion ($T>200$ K).

The derived Debye-Waller temperature $\Theta_{\mathrm{DW}}=455(8)$ K is comparable to the acoustic and calorimetric Debye temperature $\Theta_D=445-474$ K.[30] The Debye temperature has been related to the acoustic phonon modes with a cutoff frequency

$$\Theta_D=\frac{\hbar}{k_B}\left(\frac{6\pi^2N}{V_m}\right)^{1/3}\left(\frac{E}{\rho}\right)^{1/2}, \tag{9}$$

where N is the Avogadro's number, V_m is the molar volume, ρ is the density, and E is the elastic constant for acoustic wave propagation. Equation (9) has been used to derive a thermal Debye temperature Θ_D value in a range of 400–600 K depend on the choice of elastic constant (bulk, shear, or a combination). The Debye temperature Θ_D derived from acoustic approach has been demonstrated in general agreement with the derivation from the calorimetric approach using specific-heat data of the low temperatures. A mechanical interpretation of Θ_{DW} may be given by equating the thermal energy $k_B\Theta$ to the phonon energy of an atom at its resonance (Einstein) frequency, $\hbar\sqrt{E/\rho}$. The Debye-Waller temperature is thus a measure of the local atomic spring constant in microscopic point of view. It may be related to macroscopic elastic constant and heat capacity in a more general sense.

CONCLUSION

A complete thermoelastic equation of state for molybdenum has been derived from the *P-V-T* data set collected by high-*P-T* synchrotron x-ray/neutron-diffraction experiments. Different equation of state approaches, namely high-*T* EOS and thermal pressure, have been applied in the data analysis and the overall thermoelastic parameters obtained are in consistent with one another. Previous experimental data of shock wave, ultrasonic elasticity, and thermal expansion have been utilized in the global fitting of the thermoelastic equation of state of molybdenum. There are noticeable differences in the derived thermoelastic parameters when the experimental data cover a much large pressure range. However, better constraints are needed on the high-temperature related thermoelastic parameters, i.e., to greatly extend the *P-T* coverage. Thermal Grüneisen parameter has been derived for the ambient conditions and its *P-T* function could be determined if the corresponding heat-capacity data were available. The temperature derivative of bulk modulus and pressure derivative of thermal expansion of molybdenum are derived independently from the curve fittings of isothermal compression (Figs. 3 and 4), isobaric heating (Figs. 6 and 7), and elastic softening (Fig. 5), respectively. These two derivatives are comparable with one another by different approaches and can be well interpreted by a thermodynamic relationship [Eq. (6)]. The thermal vibrations of molybdenum atoms are refined from neutron-diffraction experiments are plotted as a function of pressure and temperature. Temperature has significant effect on the thermal vibrations while pressure shows little effect. The derived Debye temperature Θ_{DW}, based on the Debye-Waller factor measurement, is a thermodynamic measure of the elastic behavior of the material. It is virtually identical at high-*P-T* conditions to those derived from the low-temperature data. This indicates that the Debye-Waller temperature is an intrinsic and atom-specific property generally applicable over a wide thermodynamic *P-T* range, as demonstrated by its comparability to the acoustic and calorimetric approaches.

ACKNOWLEDGMENTS

The SAM-85/NSLS project was supported by the NSF grant for the Center for High Pressure Research (CHiPR), EAR-8920239. This work was partially performed under the auspices of the U.S. Department of Energy under Contract No. W-7405-ENG-36 with the University of California and by the Los Alamos Branch of the Institute of Geophysics and Planetary Physics, and by Los Alamos Laboratory-Directed Research and Development Funding.

[1] N. F. Fateeva and L. F. Vereshchagin, Pis'ma Zh. Eksp. Teor. Fiz. **14**, 233 (1971) [JETP Lett. **14**, 153 (1971)].

[2] R. S. Hixson, D. A. Boness, and J. W. Shaner, Phys. Rev. Lett. **62**, 637 (1989).

[3] Y. K. Vohra and A. L. Ruoff (unpublished).

[4] S. K. Sikka, B. K. Godwal, and R. S. Rao, High Press. Res. **10**, 707 (1992).

[5] W. J. Carter, S. P. Marsh, J. N. Fritz, and R. G. McQueen, NBS Spec. Publ. **36**, 147 (1971).

[6] H. K. Mao, P. M. Bell, J. W. Shaner, and D. J. Steinberg, J. Appl. Phys. **49**, 3276 (1978).

[7] D. C. Wallace, Los Alamos Scientific Laboratory Report, No. LA 12020, January, 1991 (unpublished).

[8] O. L. Anderson, *Equations of State of Solids for Geophysics and Ceramic Science* (Oxford University Press, Oxford, 1995).

[9] D. J. Weidner and SAM-85 team, High Press. Res. **8**, 617 (1992).

[10] D. L. Decker, J. Appl. Phys. **42**, 3239 (1971).

[11] Y. Zhao, D. J. Weidner, and SAM-85 team, J. Geophys. Res. **99**,

2871 (1994).
[12] A. le Bail, H. Duroy, and J. L. Fourquet, Mater. Res. Bull. **23**, 447 (1988).
[13] A. C. Larson and R. B. Von Dreele, GSAS Manual, Report No. LAUR 86-748, Los Alamos National Laboratory, 1988 (unpublished).
[14] Y. Zhao, R. B. Von Dreele, and J. G. Morgan, High Press. Res. **16**, 161 (1999).
[15] J. M. Besson, S. Klotz, G. Hamel, T. Grima, I. Makarenko, R. J. Nelmes, J. S. Loveday, R. M. Wilson, and W. G. Marshall, High Press. Res. **14**, 1 (1995).
[16] Y. Wang, D. J. Weidner, and Y. Meng, *Properties of Earth and Planetary Materials at High Pressure and Temperature*, Geophysical Monograph, Vol. 101, edited by M. H. Manghnani and T. Yagi (AGU, Washington DC, 1998), p. 365.
[17] Y. Zhao, R. B. Von Dreele, and D. J. Weidner, J. Appl. Crystallogr. **32**, 218 (1999).
[18] F. D. Murnaghan, Am. J. Math. **59**, 235 (1937).
[19] F. Birch, Phys. Rev. **71**, 809 (1947).
[20] P. Vinet, J. Ferrante, J. R. Smith, and J. H. Rose, J. Phys. C **19**, L467 (1986).
[21] P. Vinet, J. Ferrante, J. H. Rose, and J. R. Smith, J. Geophys. Res. **92B**, 9319 (1987).
[22] S. K. Saxena and J. Zhang, Phys. Chem. Miner. **17**, 45 (1990).
[23] Y. Zhao, D. Schiferl, and T. J. Shankland, Phys. Chem. Miner. **22**, 393 (1995).
[24] I. Suzuki, J. Phys. Earth **23**, 145 (1975).
[25] C. A. Swenson, J. Phys. Chem. Solids **29**, 1337 (1968).
[26] F. Birch, J. Geophys. Res. **91B**, 4949 (1986).
[27] O. L. Anderson, D. G. Isaak, and S. Yamamoto, J. Appl. Phys. **65**, 1534 (1989).
[28] G. H. Miller, T. J. Ahrens, and E. M. Stopler, J. Appl. Phys. **63**, 4469 (1988).
[29] D. I. Bolef and J. de Klerk, J. Appl. Phys. **33**, 2311 (1962).
[30] F. H. Featherston and J. R. Neighbours, Phys. Rev. **130**, 1324 (1963).
[31] J. M. Dickinson and P. E. Armstrong, J. Appl. Phys. **38**, 602 (1967).
[32] R. K. Kirby, *American Institute of Physics Handbook*, 2nd ed. (McGraw-Hill, New York, 1963), pp. 4–66.
[33] V. A. Petukhov and V. Ya. Chekhovskoi, High Temp.-High Press. **4**, 671 (1972).
[34] R. A. Rubie, B. S. Huminway, and J. R. Fisher, U. S. Geol. Survey Bull. No. 1452, Washington DC, 1978 (unpublished).
[35] R. G. McQueen and S. P. Marsh, J. Appl. Phys. **31**, 1253 (1960).
[36] B. T. M. Willis and A. W. Pryor, *Thermal Vibrations in Crystallography* (Cambridge University Press, Cambridge, 1975).
[37] H. M. Rietveld, J. Appl. Crystallogr. **2**, 65 (1969).
[38] A. C. Lawson, A. Williams, J. A. Goldstone, D. T. Eash, R. J. Martinez, J. I. Archuleta, D. J. Matinez, B. Cort, and M. F. Stevens, J. Less-Common Met. **167**, 353 (1991).
[39] J. Druyvesteyn, Physica (Utrecht) **8**, 439 (1941).